Revista Facultad de Ingeniería

Title: **Failure analysis of fractured valves for Ar-CO_2 gas storage steel cylinders**

Authors: Juan Felipe Santa-Marín, Jorge Enrique Giraldo-Barrada, Gabriel Jaime Gómez-Orrego, Marol Salomé Valencia-Calderón

DOI: **10.17533/udea.redin.20250881**

To appear in: *Revista Facultad de Ingeniería Universidad de Antioquia*

Received: January 28, 2025
Accepted: September 10, 2025
Available Online: September 10, 2025

Failure analysis of fractured valves for Ar-CO_2 gas storage steel cylinders

Análisis de falla de válvulas de cilindros para almacenamiento de Ar-CO_2

Juan Felipe Santa-Marín[1] https://orcid.org/0000-0001-5781-672X, Jorge Enrique Giraldo-Barrada[2] https://orcid.org/0000-0001-6614-0661, Gabriel Jaime Gómez-Orrego[3] https://orcid.org/0009-0004-1636-5407, Marol Salomé Valencia-Calderón[3*] https://orcid.org/0009-0006-4540-0122

[1]Grupo de Soldadura**.** Departamento de Ingeniería Mecánica, Universidad Nacional de Colombia Sede Medellín. Cra. 64c #63-120, Medellín, Colombia.
[2]Grupo de Soldadura. Departamento de Materiales y Minerales, Universidad Nacional de Colombia Sede Medellín. Cra. 64c #63-120, Medellín, Colombia.
[3]Grupo de Soldadura**.** Universidad Nacional de Colombia Sede Medellín. Cra. 64c #63-120, Medellín, Colombia.

*Corresponding author: Marol Salomé Valencia-Calderón
E-mail: marvalenciaca@unal.edu.co

KEYWORDS
Materials, corrosion, stress, gas, metallurgy.
Materiales, corrosión, esfuerzo, gas, metalurgia.

ABSTRACT: In this study, a failure analysis was conducted on two CuZn40Pb2 valves for CO_2 gas storage cylinders. The valves failed during maintenance and refilling operations performed by the operator. The investigation involved visual inspection, fractographic analysis, chemical composition determination, microstructure examination, and calculations of principal stresses and safety factors for the failed valves. The results indicated two significant issues: dezincification and stress corrosion cracking (SCC). Zinc levels near the fracture surface were found to be ten times lower than the standard value of the CuZn40Pb2 alloy, and the phenomenon was observed in both the valves and the cylinder probes. Additionally, tortuous cracks, typical of SCC, were observed near the inner threads of the valves and close to the fractured surface. These phenomena were caused by the convergence of several critical factors: moisture and/or an ion-rich environment in the system, and possible overloads due to excessive force applications. Stress calculations in two critical operational scenarios showed that tightening/loosening forces near 30 kg applied to a flowmeter could induce overload failures in the valve.

RESUMEN: En este trabajo, se realizó el análisis de falla de dos válvulas de CuZn40Pb2 para cilindros de almacenamiento de CO_2, que presentaron fractura durante operaciones de mantenimiento y rellenado de cilindros. Se realizó la inspección visual, el análisis fractográfico, la determinación de la composición

química y los cálculos de esfuerzos principales y factores de seguridad de las válvulas falladas. Los resultados indicaron dos problemas relevantes en las válvulas: descincificación y agrietamiento por corrosión bajo tensión (SCC). Se observaron valores de Zinc diez veces inferiores al valor estándar en las cercanías de la superficie de fractura y presencia del fenómeno tanto en las válvulas como en las sondas de los cilindros. Por otro lado, se observaron grietas tortuosas, típicas de SCC, en las zonas cercanas a los filetes de las roscas de las válvulas y en la zona cercana a la ruptura. Estos fenómenos ocurrieron bajo la convergencia de varios factores críticos: la humedad y/o un ambiente rico en iones en el sistema y posibles sobrecargas por la aplicación de una fuerza excesiva. Los cálculos de esfuerzos en dos casos críticos de operación mostraron que la operación con fuerzas de apriete/desapriete de un flujómetro cercanas a 30 kg pueden inducir fallas por sobrecarga en la válvula.

1. Introduction

Gas cylinder valves play a crucial role in the safety and efficient operation of industrial gas storage systems such as welding gases. According to the international standard ISO 11114-1, which provides the requirements for metallic gas cylinders and valve metal compatibility, the use of brass or copper alloy valves for Argon-CO_2 storage is acceptable and commonly employed in carbon steels or quenched and tempered steel [1].

Failures have been detected in brass components due to a degradation process known as dezincification [2]. This phenomenon occurs in moderately corrosive environments, such as alkaline solutions or chloride ion presence, leading to a selective dissolution of zinc and a porous copper surface, accelerating component deterioration [3]. Additionally, in brass plumbing system failures, Stress Corrosion Cracking (SCC) has been found as a failure mechanism, occurring due to the simultaneous presence of a corrosive environment, a material susceptible to that environment, and a tensile stress on the component. In fact, SCC initiation typically occurs at surface defects, including dealloying [4]. Consequently, these two phenomena are jointly reported in failure analysis of brass components [5] [6]. Copper-zinc alloys with more than 20% wt. zinc are particularly vulnerable to stress corrosion in the presence of ammonia or chlorides, high temperatures, and non-neutral pH water, leading to embrittlement and premature failures; heat treatments and the addition of arsenic or tin can mitigate this risk [3] [7]. On the other hand, specifically for CuZn40Pb2 alloy, both SCC and dezincification have been reported in the literature [6] [8].

In this study, a failure analysis of two yellow brass valves used for storage of Ar-CO_2 gas mixture with a CO_2 content between 12-16% wt. was done. The valves experienced sudden fracture during the refilling operations at the facilities of a gas supply company. The aim of this work is to establish the causes behind the failure of the valves through visual inspection, fractographic analysis, chemical analysis, metallographic examination, and stress calculations. The study also considered the suitability of the service and operating conditions of the valves and the material selection.

2. Materials and methods

2.1. Valves description and materials

Three (3) gas storage cylinder valves were provided by the supply gas company to be analyzed in this study: two (2) valves that failed in their respective cylinders, and one (1) valve that was operating in a cylinder during an undetermined time, which was used as a reference for a valve without any deterioration. According to the information and drawings provided by the company, both cylinders were used to store a welding Ar+CO_2 mixture with CO_2 contents between 12-16% wt. Valves material is a copper alloy CuZn40Pb2, and its reference is CGA 580-V9. This alloy contains 58% wt. Cu, 40% wt. Zn. and 2% wt. Pb and it is classified as yellow brass. The valves have two main threads: an external thread ¾”-14 NGT for the installation on the cylinder cap, and an inner thread ¼”-18 NPT for the connection of a siphon tube extending from the valve to the bottom of the cylinder. This siphon tube supplies liquid $CO_2$from the bottom of the cylinder when required. The failure occurred several months (from 3 to 6) before the failure analysis. Accordingly, the fractured surfaces deteriorated exhibiting corrosion products.

Figure 1 shows the three valves. One of the cylinders has a siphon tube, which is a sign of an operation that requires liquid CO_2. During the siphon tube disassembly, it experienced an abnormal longitudinal fracture, therefore, it was also analyzed in this work. **Figure 2** shows this component. The valve’s fracture location diagram is presented in the results section and the cracks extended from the valve inner thread to the outer thread.

Figure 1. From left to right: Valve 1 and 2 (Failed), Valve 3 (without failure).

Figure 2. Siphon tube with fitting fractured during the disassembly.

2.2. Methods

The analysis was divided into several stages: initial visual inspection, fractographic analysis, chemical composition measurements, and stress calculations during operation and valve disassembly.

2.2.1. Sample extraction

Valve 2's body was transversally cut, and the lower portion of the threaded region —containing the fracture surface —was separated and preserved intact for inspection under a stereomicroscope, as shown in **Figure 3**. The fracture surface of Valve 1 (failed) and Valve 3 were sectioned and mounted in resin to observe the fracture cross-section using optical microscope (MOP) and scanning electron microscope (SEM). **Figure 3** presents the three analyzed samples.

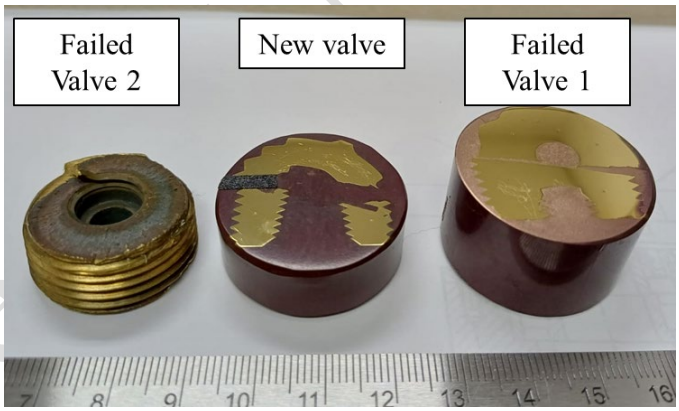

Figure 3. Samples of the analyzed valves.

2.2.2. Fractographic Analysis

Fractographic analysis was conducted according to ASTM E407 using a stereomicroscope and scanning electron microscope with a JEOL JSM7100F [9].

2.2.3. Chemical composition analysis

Chemical composition analysis was performed using a JEOL JSM7100F system coupled with an Oxford energy-dispersive spectrometry (EDS) instrument. The images from the fractured surface were taken using Backscattered Electron (BSE) in compositional mode. The correction method used for the EDS analysis was ZAF.

2.2.4. Hardness measurements

Hardness was measured using a Wolpert Universal hardness tester, according to ASTM E92 [10]. Microhardness was measured in the cross-section of valve 3 (used without failure) and Valve 1 (failed) using an INDENTEC ZHl microhardness tester by applying a 200 g load for 10 s, according to ASTM E384 [11].

2.2.5. Stress and safety factor calculation

Two cases were selected to perform the analysis and to determine the stresses in the valve, as shown in **Figure 4**. The first case involves the normal operation of the cylinder in the welding shop, with an internal pressure of around 3000 psi; an operator disassembles the flow meter, or similar, using a wrench on the external part of the valve. The second case involves the valve disassembly from the cylinder to carry the hydrostatic testing.

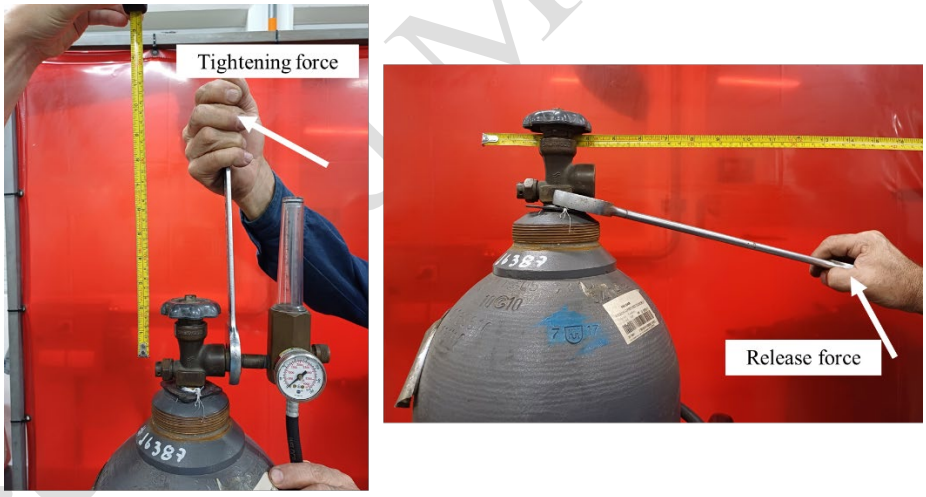

Figure 4. Cases for the analysis a) Normal operation. b) Valve disassembly.

For the safety factors calculations, a yield strength of 340 MPa is assumed, according to the typical values reported for the alloy CuZn40Pb2. The allowable tensile stress was 60% of the yield strength [12].

3. Results and discussion

3.1. Visual Inspection

Figure 5a shows the fracture surface of Valve 1 and Figure 5c shows Valve 1's remainder inside its matching cylinder. **Figure 5b** shows the fracture surface of failed Valve 2 and Figure 5d shows Valve 2's remainder in its cylinder. Fracture surfaces with different tones are clearly observed in the cross-sections. Fractographic analysis was conducted on fracture surfaces to identify possible crack initiation points and failure mechanisms indicating the root cause.

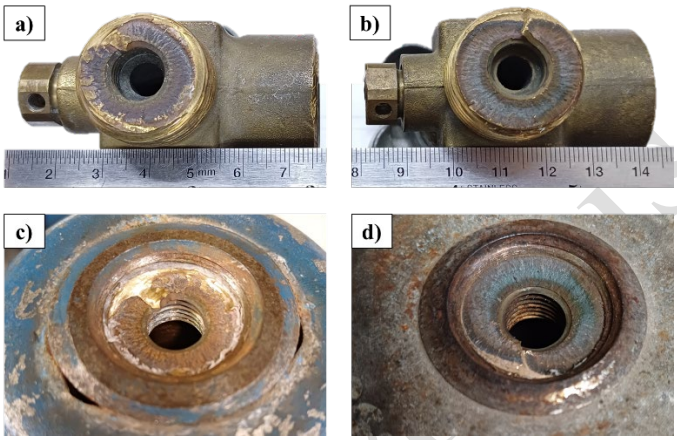

Figure 5. Failed valve's fracture surfaces.

The failure location of the two valves is presented in **Figure 6**. The failure occurred in the threaded section near the outer surface of the cylinder cap, which (i) is subjected to bending stress during operation (this will be discussed in the stress analysis section), and (ii) is exposed to contaminating elements.

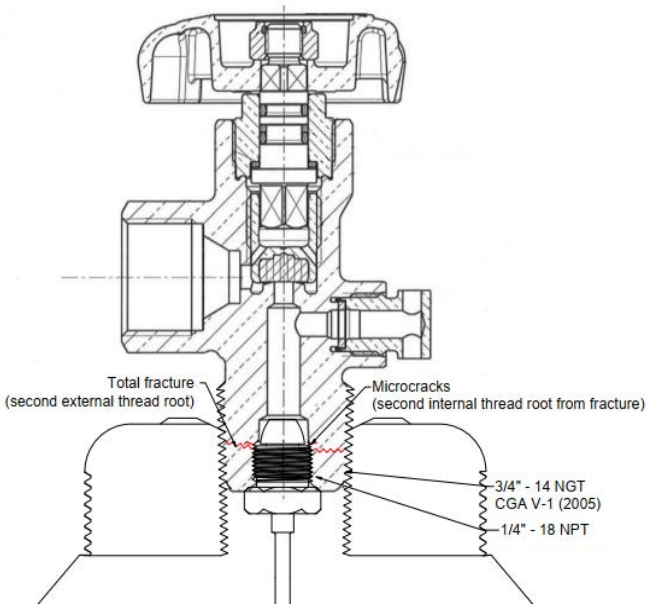

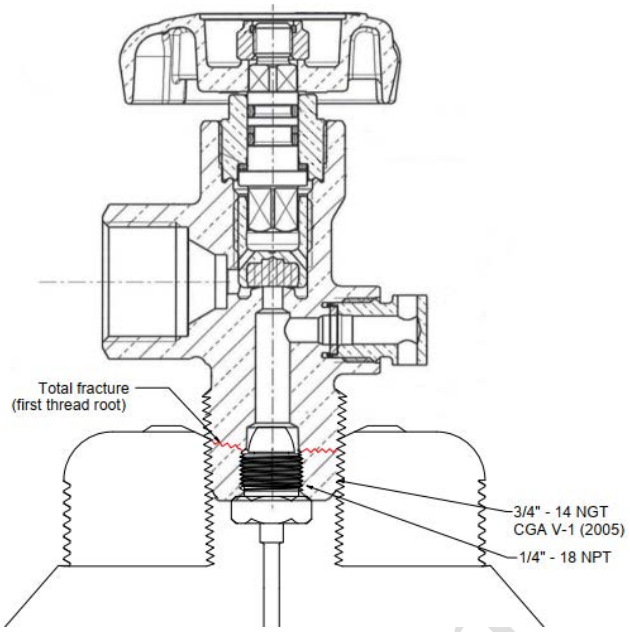

Figure 6. Fracture diagram of the analyzed valves. Valve 1 (Top). Valve 2 (Bottom).

3.2. Fractographic analysis

Figure 7 shows the appearance of the fracture surface of the failed Valve 2. The failure surface lacks markings indicating progressive failure (such as fatigue). However, different zones with varying corrosion conditions are present, as indicated by the color differences. The dark area with more advanced corrosion exhibits a reddish tone and is mainly localized at the root threads. Additionally, a yellow metallic luster is observed on the fracture surface, indicating the final rupture zone. This region shows a fractured lip, indicating the last material separation occurred with high plastic deformation. Furthermore, significant plastic deformation was evident on the threads of the two failed valves, indicating high loads during service.

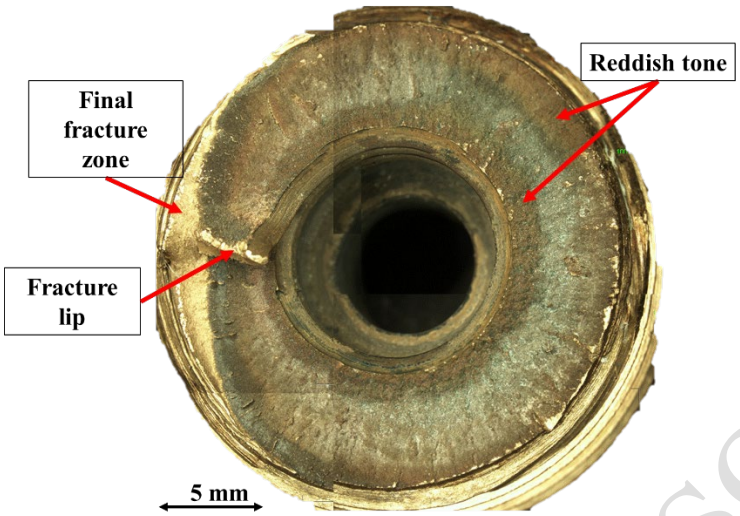

Figure 7. Failed Valve 2 fractured surface.

Observation of the fracture surface allows for conclusions to be drawn regarding several important aspects. The first significant conclusion is that different levels of corrosion were observed, indicating that the fracture progressed in multiple stages due to a possible overload, as no fatigue markings were seen. Additionally, the presence of an asymmetrical fracture lip suggests that the fracture occurred under tensile conditions of the valve. The two fractured surfaces (Valves 1 and 2) exhibit similar features, leading to the inference that both fractures follow a similar failure mechanism. This hypothesis will be confirmed later in this paper.

Figure 8 shows a micrograph of the external fracture surface of Valve 1 under an optical microscope. The fracture surface exhibits different zones with corrosion products and small cracks that propagate in a tortuous and branched manner into the material. The presence of these cracks and corrosion products on the fracture surface is uncommon in failures of metallic elements subjected to pure mechanical loads without significant environmental influence, serving as clear evidence that the fracture resulted from interaction with a medium that altered the base material of the valve [4].

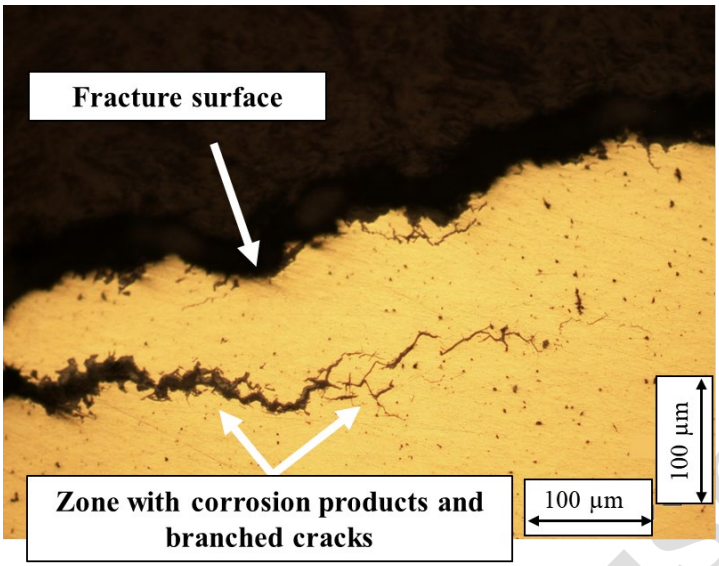

Figure 8. Fracture zone detail of failed Valve 1.

Figure 9 shows the longitudinal cross-section of the inner threads of failed Valve 1 (thread ¼”-18 NPT), observed under an optical microscope. Cracks are observed at the roots of the internal threads of the valve, propagating from inside (see **Figure 9a** and **9b**). The appearance of these cracks is very similar to those found on the fracture surface of the valve (see **Figure 9c** and **9d**). Additionally, the presence of pores or pits in regions near the cracks is observed (see **Figure 9e** and **9f)**. The tortuous and branched cracks with corrosion products can be clear evidence of SCC as reported by other authors [13]. **Figure 10** shows a micrograph of the etched thread cross-section. Reddish zones are observed due to dezincification [5]. **Figure 11** exhibits deformed grains on thread fillets.

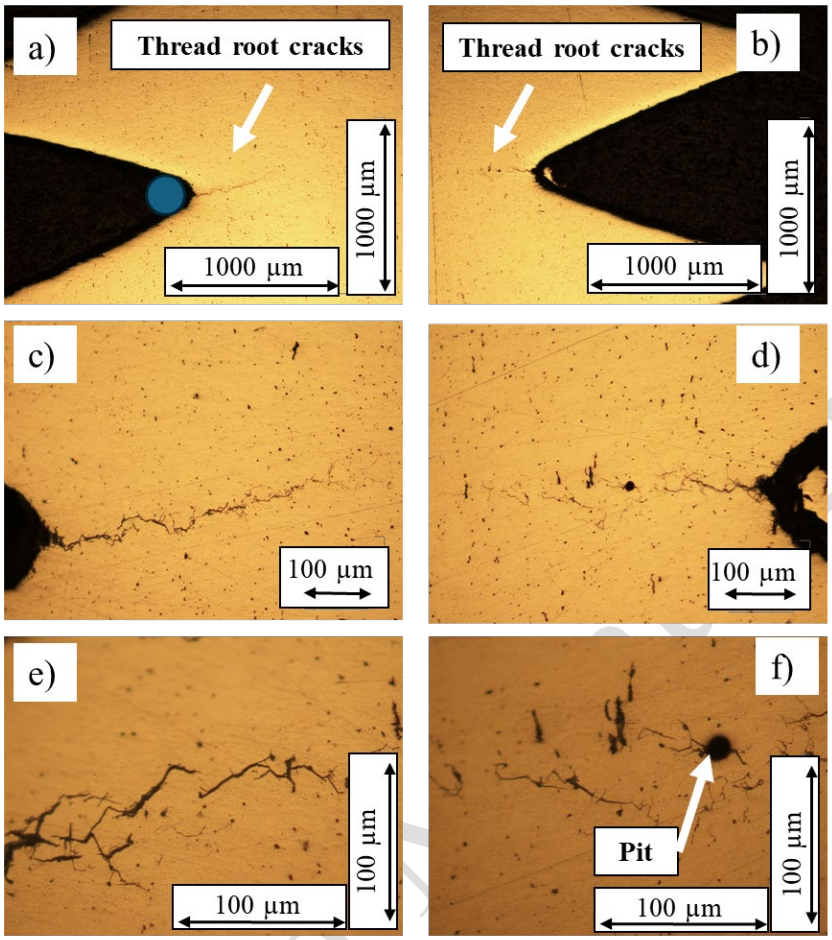

Figure 9. Cross-section of the inner threads of failed Valve 1. Optical microscope.

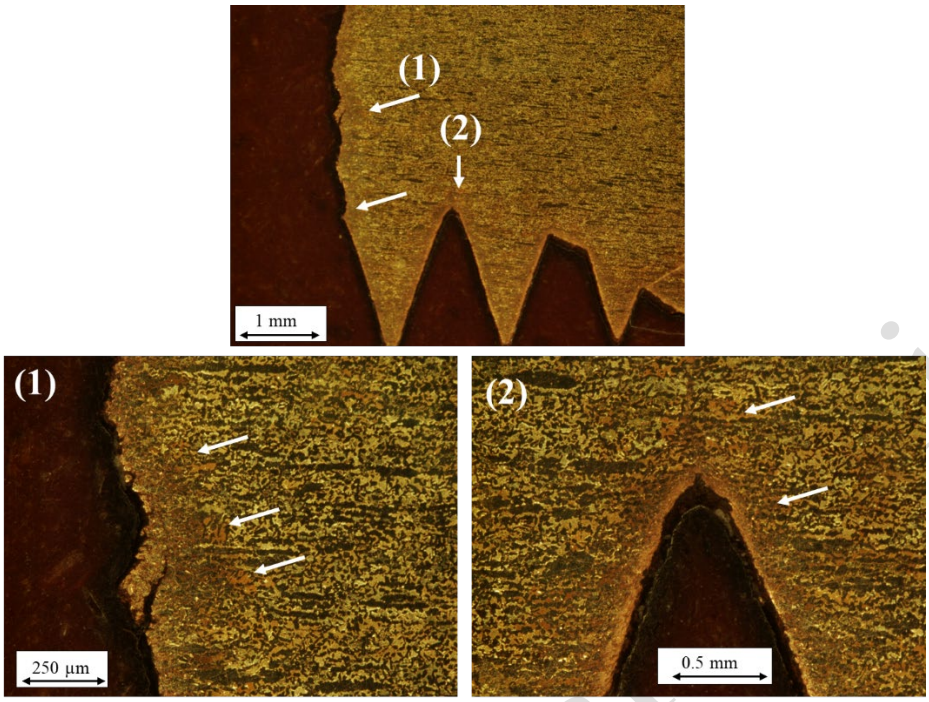

Figure 10. Reddish zones around inner thread cross-section.

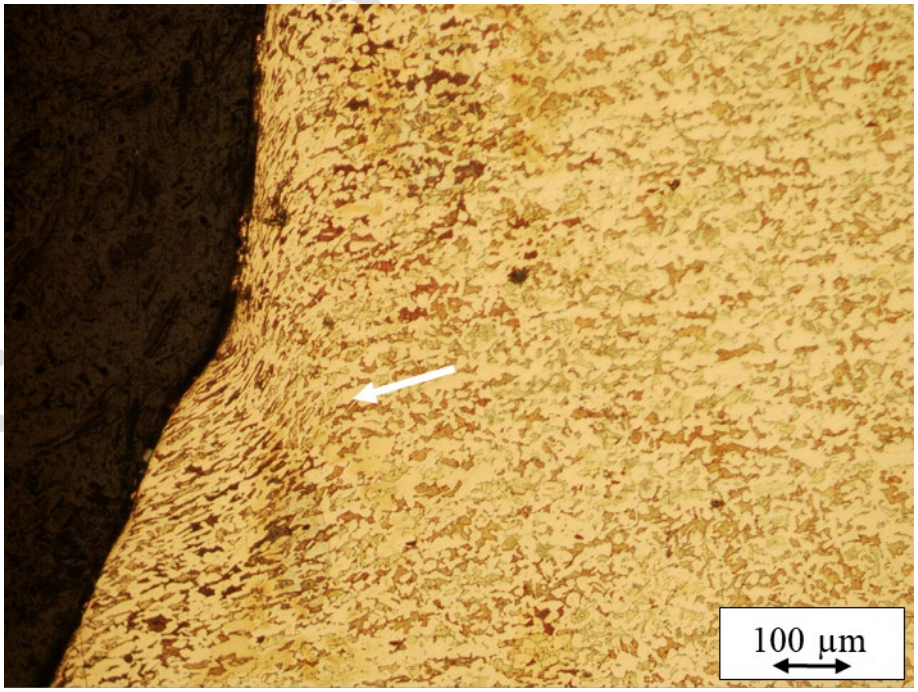

Figure 11. Deformed grains near failure zone

3.3. Chemical microanalysis and Electron Microscopy

Additional inspection of the failed Valve 1 and the fractured siphon tube using chemical microanalysis and electron microscopy revealed an additional issue of high importance for the analysis. **Figure 12** shows images of the cross-section of the fracture surface observed under the scanning electron microscope. In **Figure 12**, the corrosion products, previously shown in **Figure 8**, are visible. Here, using backscattered electron microscopy, qualitative changes in the chemical composition of the material can be observed. A high amount of bright white particles, corresponding to lead particles, is observed, which is expected in these alloys because Pb is added to improve machinability. Additionally, dark gray zones with corrosion products are seen in the fracture section (right of **Figure 12**), indicating a different chemical composition from the base material. Furthermore, **Figure 12** shows the area near the fracture exhibiting significant porosity or pitting.

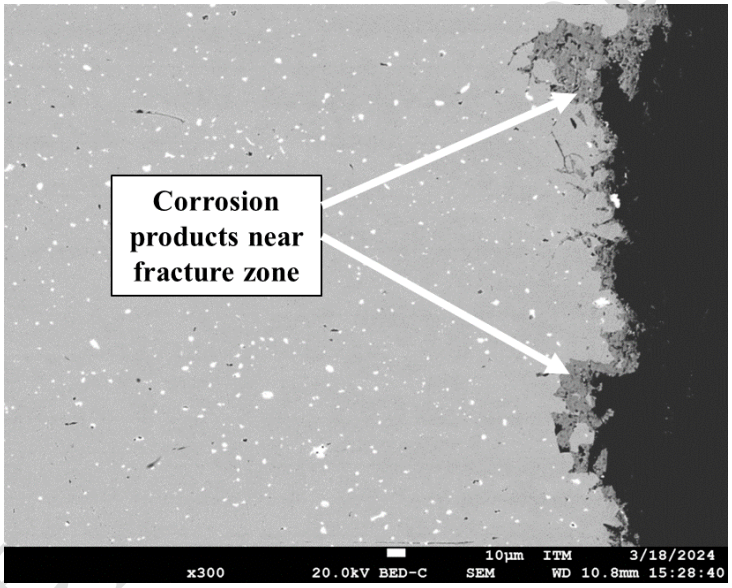

Figure 12. Cross-sectional surface of failure observed in scanning electron microscope.

Figure 13 shows the results of the measurements of the chemical composition in a deteriorated zone (corroded area near the fracture) and in a nearby undeteriorated zone. The quantitative results are presented in the table attached to the same image. The results indicate that the deteriorated zone has significantly lower zinc levels compared to the expected values for the alloy. It is noted that in an undeteriorated zone, the zinc levels are between 35% wt. and 40% wt., while in the deteriorated zones, they are close to 2% wt. This result was supplemented by a qualitative linear analysis through the deteriorated zone, shown in **Figure 14**. The results showed that inside the areas with corrosion products, the amount of zinc significantly decreased to close to one-tenth (from 37% wt. to 2% wt.) of the average values in the undeteriorated zone.

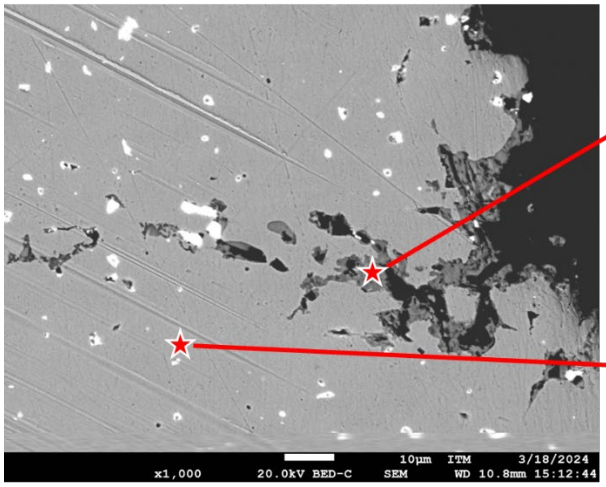

Deteriorated zone	
Element	Wt%
O	20.80
Cu	76.99
Zn	2.20
Total:	100.00

Zone without deterioration	
Element	Wt%
Cu	62.17
Zn	37.83
Total:	100.00

Figure 13. Chemical composition analysis in the deteriorated zone and the undeteriorated zone.

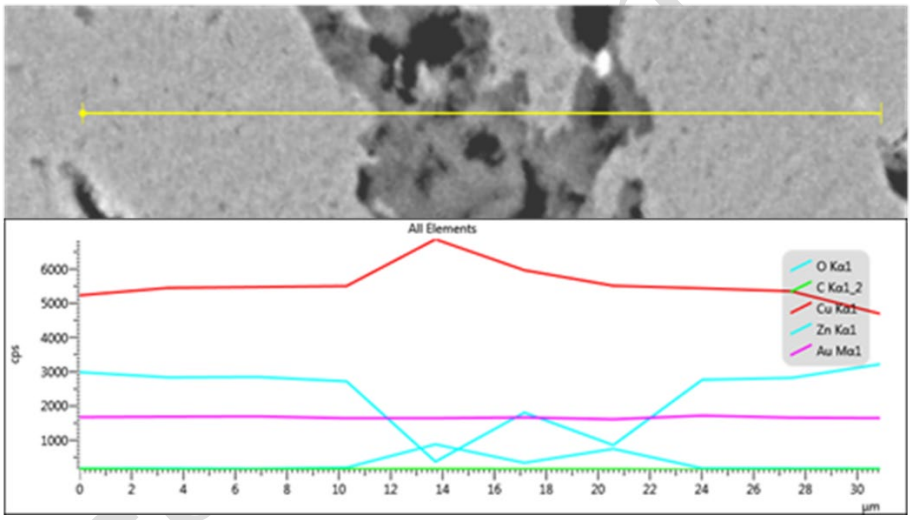

Figure 14. Linear analysis of element variation from an undeteriorated zone to a cracks and internal oxides zone.

According to the results obtained in this section, it can be concluded that the analyzed samples also exhibit the phenomenon of dezincification. In these alloys (CuZn40Pb2), corrosion can lead to the loss of the most reactive component of the yellow brass alloy (zinc), leaving behind the less reactive component. The general terms for this process are 'dealloying', 'selective corrosion', or 'selective leaching'. Specifically, the term 'dezincification' is used for the loss of zinc [3].

Since dezincification was found in Valve 1 (failed), an analysis was conducted on the anomalously fractured siphon tube. **Figure 15** shows the failed siphon tube and the analysis of the fracture surfaces. This element is of high importance for the analysis, as it is made from a material similar to the valve

(CuZn40Pb2). Since the siphon tube was exposed to the same environment inside the cylinder, it should exhibit the same phenomenon of decreased zinc content on its surface.

The micrographs taken with the electron detector, sensitive to changes in chemical composition (BEC) or (BSE) back-scattered electrons in compositional mode, clearly show the presence of different chemical composition along the thickness of the siphon tube. This zone is recognized by the presence of dark grey zones. An example of the chemical composition in these areas is also shown in **Figure 16**. The previous results indicate that the siphon tube connected to the fitting also exhibits the phenomenon of dezincification, leading to its brittle fracture. The dark gray areas are preferentially observed (see **Figure 15**) in the internal region of the siphon tube (zinc-rich areas). Also, green stains indicating copper corrosion products are observed on the internal surface of the siphon tube.

Summarizing, the evidence indicates that the siphon tube also experienced dezincification. This phenomenon caused the anomalous brittle rupture during disassembly. The authors consider that copper corrosion and simultaneous dezincification could indeed occur. However, since the handling of the sample by the company involved in the failure analysis is unknown, it is impossible to determine the exact timing of this phenomenon. It is noteworthy that dezincification and copper corrosion products preferentially appear in the internal area of the siphon tube, which may be due to the condensation of water vapor caused by the gas flow within the siphon tube and fitting.

Finally, the authors verified that dezincification occurred in both valves. The unmodified fracture surface of failed Valve 2 was examined, and a chemical analysis was performed using the electron microscope. The red zone indicated in section 3.2 revealed the presence of areas with high zinc content (see **Figure 17**). These same areas have been documented in the literature as 'meringue' and were observed on the surfaces of the cylinder threads [3]. This result indicates that the dezincification phenomenon was also observed in both independent failure events.

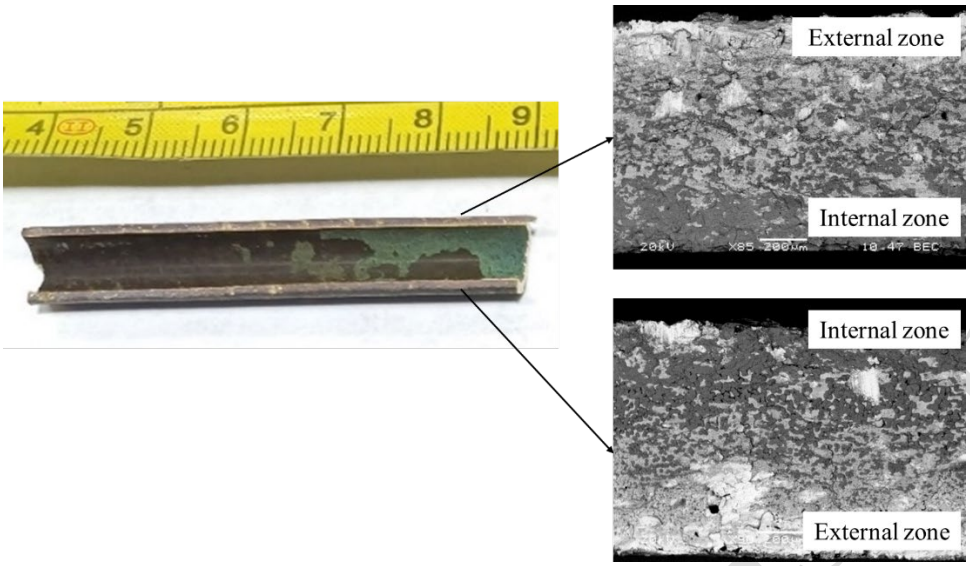

Figure 15. Qualitative chemical analysis of abnormal fractured siphon tube with dezincification evidence.

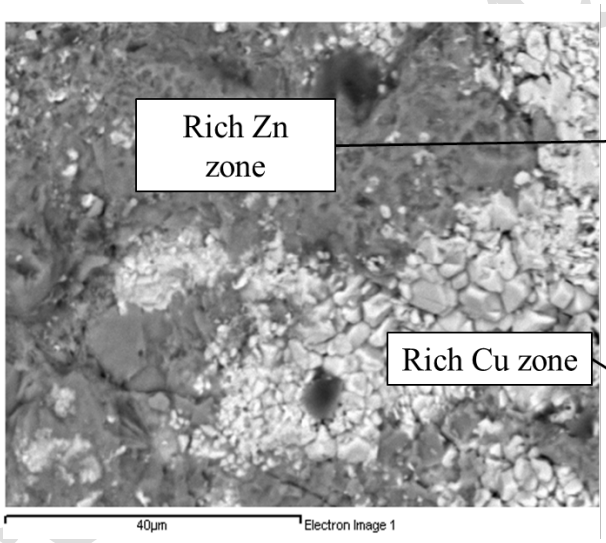

Element	Weight%
O K	29.56
Cu K	15.34
Zn K	55.10
Totals	100.00

Element	Weight%
O K	1.15
Cu K	91.64
Zn K	7.21
Totals	100.00

Figure 16. Siphon tube dezincification zones.

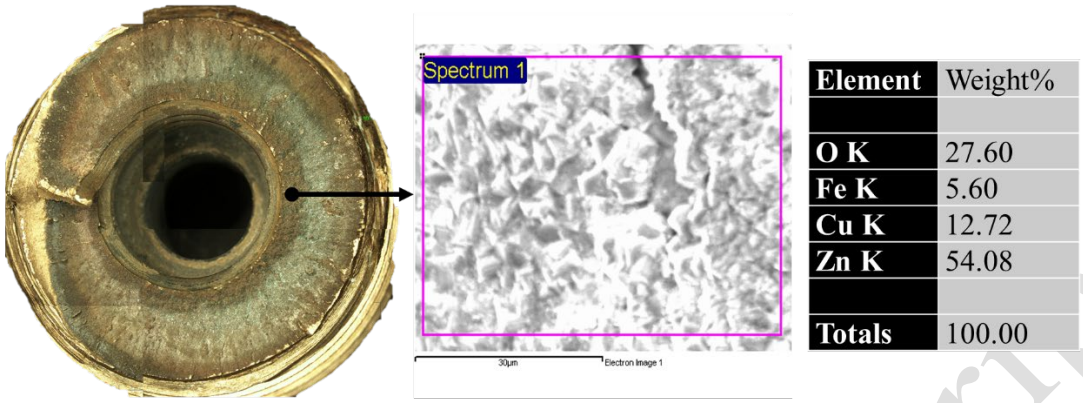

Figure 17. Chemical analysis in fractured zone with high zinc content areas.

3.4. Chemical composition and hardness measurements

Table 1 shows a summary of the results of the chemical composition of the material from both failed valves, as measured by the electron microscope. The table also includes the standard chemical composition for CW617N (CuZn40Pb2) [12] and the hardness of samples.

Table 1. Chemical composition measured by energy dispersive spectroscopy and hardness.

Sample	Cu % wt.	Zn % wt.	Pb % wt.	Hardness (HV)
Valve with no failure	58.6	40.3	1.1	117±2
Failed Valve 2	58.1	40.0	1.7	110±2
CuZn40Pb2	57-59	Rem.	1.6-2.5	120

The results indicate that the chemical composition of both valves matches the specified composition for this brass alloy. Additionally, the hardness values of the undamaged valve are consistent with those reported for CuZn40Pb2.

The microhardness of samples was measured in the cross-section of the undamaged valve and failed Valve 1, using a 200 g load for 10 s. The valve with no failure has 129±4 HV, while the failed sample in a distant zone showed 120±4 HV. These values align with macrohardness readings and are slightly higher due to lower load effects. However, near the failure zone, the failed sample registered values of 177±2 HV and 146±3 HV at approximately 50 microns from the external thread surface of the fracture. This increase of hardness is typical in brass alloys with high work hardening, indicating high deformation near the fracture zone. This suggests possible excessive forces during valve operation, leading to these deformations, with the hardness increase potentially indicating an overload during failed valve operation.

3.5. Stress and safety factor calculations

3.5.1. Case 1: Normal operation

In the first case, the valve is subjected to torsional and bending moments from the applied force shown in **Figure 4a,** when the flowmeter is connected. Additionally, the valve thread endures tensile stress due to internal gas pressure. This internal pressure decomposes into two main forces generating tensile stress in the valve's threaded region where failure occurred. The force on the valve stem's internal surface (F1 in **Figure 18**) reaches 67 kgf, derived from an internal pressure of 3000 psi over a ¼" diameter circle. The force F2 achieves 1004 kgf from a 3000 psi pressure over an area with a 1" outer diameter and a ¼" inner diameter. Thus, the resultant tensile force reaches 1071 kgf, producing a tensile stress of 22.5 MPa, excluding stress concentrations from the threads.

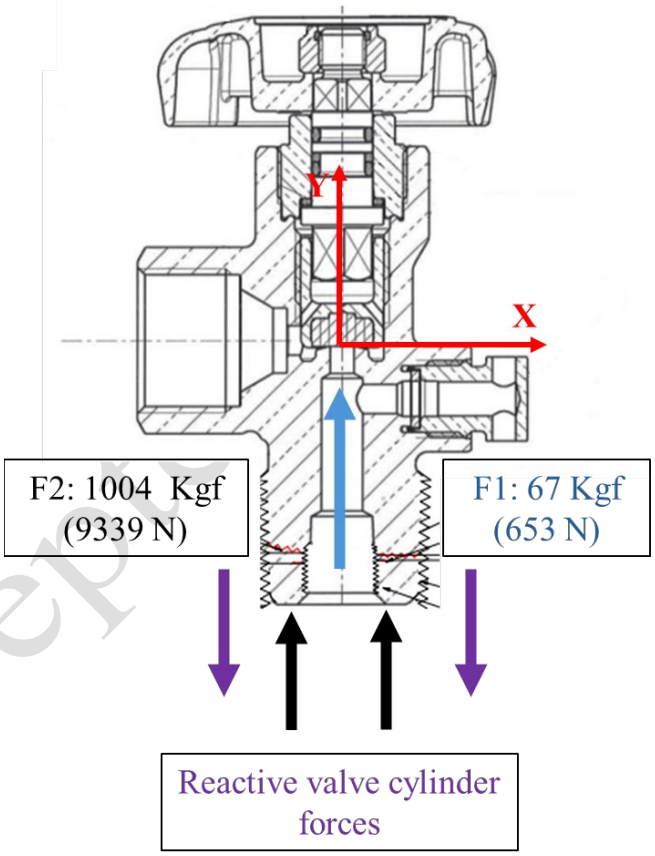

Figure 18. Free body diagram for forces generated by internal gas pressure.

The force applied by the operator creates a bending moment, calculated by multiplying a 30 kgf force with a 35 cm lever arm (see wrench diagram in **Figure 4**), resulting in a bending moment (M) of 103

Nm. This bending moment, using **Equation 1**, produces a bending stress on the valve surface reaching 64 MPa, with a c value of 12.7 mm and a moment of inertia (I) of 20351 mm⁴.

$$\sigma_f = \frac{M \cdot c}{I} \quad (1)$$

This stress value has the same direction of the tensile stress generated by internal pressure, yielding a total normal stress of 86.5 MPa. A stress concentration factor will correct the total normal stress due to the section change in the failure zone. Using values of r = 0.27 mm, D = 27 mm, and d = 24 mm, and applying the case of a groove under bending, a flexural stress concentration factor (k_1) of 2.5 is obtained. The radius was measured in the thread cross-section and verified against the ISO 5145:2017 standard, which specifies a 0.274 mm radius [14]. Using **Equation 2**, a total bending stress of 216 MPa is obtained.

$$\sigma_T = k_1 \cdot \sigma_f \quad (2)$$

Additionally, the operator's tightening force generates a shear stress from torsion, originating from a torque (T) of 11.7 Nm due to a 30 kgf force applied over a 40 cm arm. This torsional stress, calculated with **Equation 3**, reaches 3.65 MPa using a radius (c) of 12.7 mm and a polar moment of inertia (J) of 40703 mm^4.

$$\tau_1 = \frac{T \cdot c}{J} \quad (3)$$

These stresses require adjustment with a torsional stress concentration factor (k_2 = 1.7), applied through **Equation 4**, resulting in a corrected shear stress value of 6.2 MPa.

$$\tau = k_2 \cdot \tau_1 \quad (4)$$

The calculated safety factor, based on the Von Mises stress, reaches a value of 1.48, assuming a yield strength of 340 MPa. This assumption aligns with hardness values reported in the catalog and with measured values, as tensile strength measurements could not be performed due to sample geometry constraints [12].

3.5.2. Case 2: Valve disassembly

During the valve removal for hydrostatic testing of the cylinder (**Figure 4b**), a force of 30 kgf is applied at 30 cm, generating a torsional moment (T) of 88 Nm. The resulting shear stress, calculated using **Equation 3**, is 27.5 MPa. After applying a concentration factor (k_2 = 1.7) through **Equation 4**, the corrected shear stress is 46.8 MPa. Additionally, this force generates a bending moment (M) of 11.8 Nm, resulting in a bending stress of 7.3 MPa, calculated using **Equation 1**. After correcting the value with **Equation 2**, the bending stress reaches 18.5 MPa. Consequently, the safety factor for this case is 4.09.

Summarizing, after the stress analysis, it can be concluded that the component is designed to withstand the loads in the two cases analyzed in this report. However, this analysis does not include elements such as impulsive loads generated by impacts during valve operation. Additionally, wrenches larger than those assumed in this report or impacts during disassembly could cause overloads due to the relatively low safety factors.

4. Discussion

The analysis of three fractured surfaces (two valves and the siphon tube) showed that the dezincification phenomenon was evident in all of them.

Valve 1 had evidence of SCC (**Figure 9**). SCC occurs when three conditions are present: the presence of a corrosive environment, the material's susceptibility to that environment, and mechanical stress applied to the component [4] [8]. The valves were subjected to stress generated by the internal gas pressure and/or stress produced during the assembly or disassembly of the valve during hydrostatic testing of the cylinders.

The sources of moisture in the cylinder are unknown. The authors did not have access to the cylinders' history, making it impossible to confirm the sources of moisture, chlorides, or ammonium. However, remnant water from hydrostatic tests and humidity in the gases due to improper use or storage of the cylinders is possible. No residues of ammonium salts and/or chlorides were detected in the chemical analysis. However, these sources of ions are common in everyday applications. Ammonium salts were frequently used during the pandemic for disinfecting surfaces, while chloride-rich environments are common in coastal cities.

The evidence from the three fractured surfaces analyzed is conclusive. These two corrosion events altered the chemical composition and strength of the valve material and were decisive in the failure.

Regarding the material selection for the valve, it should be noted that, although the material is susceptible to dezincification and SCC whenever the previously described environment is present, as specified in the technical data sheet [12], valve material does not contain stabilizing elements reported in the literature to prevent these phenomena [3]. Also, valve material hardness reaches values above 115 HB, which is higher than the recommended limit to prevent SCC [15]. However, this alloy has been traditionally used for this valve.

On the other hand, there are some indications regarding possible overload. The first one is located on the fracture surface, where a metallic yellow-shine zone is observed, indicating the final fracture zone. This region exhibited a fracture lip, marking the location of the last material detachment accompanied by high plastic deformation (see **Figure 7**). Additionally, the thread fillets of both failed valves showed

significant plastic deformation, suggesting the presence of high operational loads during service (see **Figure 11**).

Based on the previous evidence, a primary failure cause and secondary failure causes were proposed. The primary cause of the failure is related to the fact that service conditions of the valves were different from the design conditions. The presence of moisture and/or a chloride-rich environment led to dezincification, stress corrosion, and subsequent rupture when stresses were applied during valve installation or removal. A secondary failure cause is also proposed: the possible overload due to excessive force application.

5. Conclusions

The analysis of three fractured surfaces (two valves and the siphon tube) showed that the dezincification phenomenon was evident in all of them. This phenomenon has been reported for the same material of the valves (CuZn40Pb2) and results in zinc-rich deposits on the surfaces of components exposed to environments that promote this type of corrosion [3] [8]. Low resistance to dezincification is reported when this material is exposed to water, humid atmospheres, or solutions containing chloride ions, such as seawater [12] [16] [17]

Valve 2 had evidence of SCC. SCC occurs when three conditions are present: the presence of a corrosive environment, the material's susceptibility to that environment, and mechanical stress applied to the component [4] [8].

The main reason for the failure is that the service conditions of the valves differed from the intended design conditions. The presence of moisture and/or an environment rich in chlorides or ammonium resulted in dezincification, stress corrosion, and eventual rupture when stresses were applied during the installation or removal of the valves. A secondary failure cause is also proposed: the possible overload due to excessive force application

6. Declaration of Competing Interest

We declare that we have no significant competing interests including financial or non-financial, professional, or personal interests interfering with the full and objective presentation of the work described in this manuscript.

7. Acknowledgement

The authors would like to acknowledge to the Laboratorio de Tecnología y Diseño de Materiales and Laboratorio de Soldadura from Universidad Nacional de Colombia for their support to analyze the

samples. Electron Microscopy laboratory from Instituto Tecnológico Metropolitano is also acknowledged.

8. Author contributions

J. F. Santa-Marín: Supported fractography and electron microscopy. J. E. Giraldo-Barrada: Contributed to chemical analysis and light optical microscopy. G. J. Gómez-Orrego: Performed visual inspections and conducted hardness measurements. M. S. Valencia-Calderón: Carried out stress calculations and reviewed articles for the introduction and state of the art sections. All authors contributed to results analysis and synthesis and paper writing.

9. Data availability statement

The data that supports the findings of this study is available from the corresponding author upon reasonable request

10. References

[1] International Organization for Standarization, "ISO 11114-1:2020. Gas cylinders — Compatibility of cylinder and valve materials with gas contents. Part 1: Metallic materials," 2020, *Geneva*.

[2] A. Pelto-Huikko, N. Salonen, and M. Latva, "Dezincification of faucets with different brass alloys," *Eng Fail Anal*, vol. 169, p. 109202, Mar. 2025, doi: 10.1016/j.engfailanal.2024.109202.

[3] Y. Zhang, "Dezincification and Brass Lead Leaching in Premise Plumbing Systems: Effects of Alloy, Physical Conditions and Water Chemistry," Virginia Polytechnic Institute and State University, Blacksburg, 2009.

[4] V. Očenášek and J. Luštinec, "Stress Corrosion Cracking and Copper Alloy Products," *Manufacturing Technology*, vol. 22, no. 1, pp. 39–44, Feb. 2022, doi: 10.21062/mft.2022.012.

[5] G. Pantazopoulos, "A review of defects and failures in brass rods and related components," *Practical Failure Analysis*, vol. 3, no. 4, pp. 14–22, Aug. 2003, doi: 10.1007/BF02715925.

[6] G. A. Pantazopoulos and A. I. Toulfatzis, "Failure analysis of a machinable brass connector in a boiler unit installation," *Case Stud Eng Fail Anal*, vol. 1, no. 1, pp. 18–23, Jan. 2013, doi: 10.1016/j.csefa.2012.11.002.

[7] W. Reitz, "Failure analysis of brass bolt from mausoleum," *Journal of Failure Analysis and Prevention*, vol. 5, no. 4, pp. 20–25, Aug. 2005, doi: 10.1361/154770205X55126.

[8] E. Brandl, R. Malke, T. Beck, A. Wanner, and T. Hack, "Stress corrosion cracking and selective corrosion of copper-zinc alloys for the drinking water installation," *Materials and Corrosion*, vol. 60, no. 4, pp. 251–258, Apr. 2009, doi: 10.1002/maco.200805079.

[9] ASTM International, "E407-23. Practice for Microetching Metals and Alloys," Nov. 01, 2023, *ASTM International, West Conshohocken, PA*. doi: 10.1520/E0407-23.
[10] ASTM International, "E92-23. Test Methods for Vickers Hardness and Knoop Hardness of Metallic Materials," Jul. 01, 2023, *ASTM International, West Conshohocken, PA*. doi: 10.1520/E0092-23.
[11] ASTM International, "E384-22. Test Method for Microindentation Hardness of Materials," Oct. 01, 2022, *ASTM International, West Conshohocken, PA*. doi: 10.1520/E0384-22.
[12] Nordic Brass, "BRASS ALLOY CW617N," Jul. 2019. Accessed: Mar. 17, 2024. [Online]. Available: https://www.nordicbrass.se/download/200-C0D29696FC1EEA771DF60FF95A4772FF/CW617N_Stang_eng_utg-3.pdf
[13] M. Vakili, P. Koutník, J. Kohout, and Z. Gholami, "Analysis, Assessment, and Mitigation of Stress Corrosion Cracking in Austenitic Stainless Steels in the Oil and Gas Sector: A Review," *Surfaces*, vol. 7, no. 3, pp. 589–642, Aug. 2024, doi: 10.3390/surfaces7030040.
[14] International Organization for Standarization, "ISO 5145:2017. Gas cylinders — Cylinder valve outlets for gases and gas mixtures — Selection and dimensioning," 2017, *Geneva*.
[15] H. Sugawara and H. Ebiko, "Dezincification of brass," *Corros Sci*, vol. 7, no. 8, pp. 513–523, Jan. 1967, doi: 10.1016/S0010-938X(67)80090-8.
[16] Walther praezision, "walther-praezision." Accessed: Mar. 17, 2024. [Online]. Available: https://www.walther-praezision.de/en/entzinkung-von-messing-oder-selektive-korrosion/
[17] A. Cohen, "Corrosion of Copper and Copper Alloys," in *Corrosion: Materials*, ASM International, 2005, pp. 125–163. doi: 10.31399/asm.hb.v13b.a0003816.